Journal of Nuclear Materials 379 (2008) 105–111

Contents lists available at ScienceDirect

Journal of Nuclear Materials

journal homepage: www.elsevier.com/locate/jnucmat

# Study of archaeological artefacts to refine the model of iron long-term indoor atmospheric corrosion

J. Monnier [a,b,*], L. Legrand [c], L. Bellot-Gurlet [d], E. Foy [a], S. Reguer [e], E. Rocca [f], P. Dillmann [a,g], D. Neff [a], F. Mirambet [h], S. Perrin [i], I. Guillot [b]

[a] Laboratoire Pierre Süe – UMR 9956 CEA-CNRS, bât 637 CEA Saclay, 91191 Gif-sur-Yvette, France
[b] Institut de Chimie des Matériaux de Paris Est-équipe MCMC, UMR 7182 CNRS-Université Paris 12, 2-8 rue Henry Dunant, 94320 Thiais, France
[c] Laboratoire Analyse et Modélisation pour la Biologie et l'Environnement, UMR 8587, Evry, France
[d] Laboratoire de Dynamique, Interaction et Réactivité (LADIR), UMR 7075 CNRS and Université Pierre et Marie Curie Paris 6, 2 rue Henry Dunant, 94320 Thiais, France
[e] Synchrotron SOLEIL, Saint-Aubin BP 4891192 Gif-sur-Yvette, France
[f] Laboratoire de Chimie du Solide Minéral, UMR 7555, Université Henri Poincaré-Nancy I, France
[g] IRAMAT UMR 5060, IPSE – CEA Saclay, Gif-sur-Yvette, France
[h] Laboratoire de Recherche des Monuments Historiques, 29, rue de Paris, Champs-sur-Marne, France
[i] Laboratoire d'Etude de la Corrosion Aqueuse, SCCME, bât 458 CEA Saclay, 91191 Gif-sur-Yvette, France

A B S T R A C T

The study of long-term indoor atmospheric corrosion is involved in the field of the interim storage of nuclear wastes. Indeed study of archaeological artefacts is one of the only mean to gather information on very long periods. Concerning ancient items, due to the complexity of the system, it is necessary to couple many analytical techniques from the macro to the microscopic scale. This enables to propose a description of the Amiens cathedral chain rust layers, made of a matrix of goethite, with lepidocrocite and akaganeite locally present and marbling of a poor crystallized phase associated to ferrihydrite. Electrochemical measurements permit to study the reduction capacity of the rust layer and to draw reduction mechanisms of the so-called active phases, by *in situ* experiments coupled with X-ray diffraction and X-ray absorption spectroscopy.



## 1. Introduction

The apprehension of iron long-term indoor atmospheric corrosion mechanisms is of great importance in the French nuclear waste management context. Indeed, vitrified wastes could be embedded in low alloy steel overpacks. After a short period of dry corrosion and a temperature decrease, the overpack will be exposed for several centuries to indoor atmospheric corrosion conditions [1]. Therefore, the long-term corrosion mechanisms of these materials have to be understood for periods of several hundred years, in order to predict the degradation behaviour of the overpacks.

Numerous data are available on outdoor short-term processes, including quite long exposure periods (i.e. over 10 years). Results from a number of testing show that the behaviour of low alloy steels or iron can be characterized by two parameters $K$ and $n$ as far as a power law between penetration $P$ and time $t$ (i.e. $P = K \cdot t^n$) is valid for outdoor conditions. Although these laws are helpful in extrapolating results of corrosion tests over a few ten years, they are not reliable enough for the very long-term predictions (a few hundred years) required for interim storage of nuclear wastes. Moreover, this latter approach is not adapted to predict the reactivity of the corrosion layers developed on very long periods as the ones concerned by the frame of the nuclear waste interim storage. As a consequence, complementary to laboratory simulation on coupons and numerical modelling, it is crucial to study the corrosion layers of heritage artefacts submitted to indoor atmospheric corrosion for several hundred years. This kind of study should help refining the available model also based on laboratory measurements and simulations.

As demonstrated by Evans and Taylor [2], long-term atmospheric corrosion mechanisms are controlled by the wetting and the drying of water on the artefact. These evolutions are drawing a so-called wet–dry cycle that depends on the environmental conditions on site but also on the metallic artefact size. Depending on the relative humidity (RH) of the atmosphere and the temperature evolution, a water film will form and disappear on the metallic surface. When the cycle occurs, the corrosion can start, summarized by the following equation:

$$4Fe + 2H_2O + 3O_2 \rightarrow 4FeOOH. \quad (1)$$

This general equation points out that the iron, the electrolyte and an oxidant have to be present at the same time to observe a

* Corresponding author. Address: Laboratoire Pierre Süe – UMR 9956 CEA-CNRS, bât 637 CEA Saclay, 91191 Gif-sur-Yvette, France. Tel.: +33 1 69 08 23 05; fax: +33 1 69 08 69 23.
*E-mail address:* judith.monnier@cea.fr (J. Monnier).

0022-3115/$ - see front matter © 2008 Elsevier B.V. All rights reserved.
doi:10.1016/j.jnucmat.2008.06.008

corrosion process. The rust formed is in reality a complex layer, made up of several mixed phases. The most commonly reported phase is goethite (α-FeOOH) [2]. Lepidocrocite (γ-FeOOH) and akaganeite (β-FeOOH) were also detected [3]. Although these three iron oxy-hydroxides have the same chemical formula, they present different crystallographic structures that can be differentiated. Moreover akaganeite contains about 7 wt% chlorine in its structure [4]. In addition to these phases, iron oxides magnetite ($Fe_3O_4$) and maghemite ($\gamma$-$Fe_2O_3$) are also reported [5]. These crystallized phases are identified in the corrosion products by X-ray diffraction (XRD) and micro X-ray diffraction (μXRD) methods. More recently, using Raman micro spectrometry and micro-X-ray absorption spectroscopy (μXAS) under synchrotron radiation, less crystallized phases have been detected such as feroxyhite (δ-FeOOH) and/or a type of ferrihydrite, a hydrated oxy-hydroxide that can be present under two forms according to literature [6,7].

The wet/dry cycle can be divided into three stages. During its first stage, named the 'wetting stage', a water film forms on the surface of the sample. During this step, it can be shown that iron consumption is much higher than oxygen one [8]. Thus, to let the oxidation reaction responsible for iron consumption occur, another phase of the system should be reduced. Experiments made on rusted iron coupons [9] proved that the rust layer contains at least one of such phases that are able to be reduced, and can act in the corrosion processes. Stratmann and Hoffmann [9] hypothesized that the active phase is lepidocrocite that could be reduced to Fe·OH·OH. These results were the basements of the phenomenological model of atmospheric corrosion developed by Hoerlé et al. [10].

Yamashita et al. [11] only identified lepidocrocite and goethite, respectively considered as active and stable. Kihira et al. [12] introduced amorphous phases, but stated that they are stable ones. He also defined magnetite as active. On the contrary, Hoerlé et al. [10] considered magnetite as a stable phase. It appears that this point is not so far clear. In fact, other works studying electrochemical reactivity of reference phases that could be present in the rust layer [13] revealed that each of them can have very different reactivities. Consequently, different groups with the same electrochemical behaviour can be defined. Magnetite, maghemite and goethite are considered as non-reactive phases. A second group of reactive phases is constituted by lepidocrocite, ferrihydrite and feroxyhite.

It appears that it is necessary on the one hand to perform a fine characterization of ancient corrosion layers to determine precisely what are the constituting phases of the rust layers, and on the other hand to study the reactivity of these rust layers in function of their composition. Last but not least it is also important to precise the behaviour of these reactive phases during the wet/dry cycle.

To answer these questions, three axes were followed in the present study. Firstly, a fine characterization of multisecular corrosion layer sampled on an historical building using micro-focused coupled techniques was realized, in order to confirm what phases are present and what their respective proportions in the rust layer are. Secondly, the electrochemical behaviour of the corrosion layer itself was studied and compared to the one of other ancient historical samples. Eventually, electrochemical measurements were coupled with *in situ* structural characterization, in order to investigate reduction mechanisms of the different active phases occurring during corrosion processes controlled by the wet–dry cycle.

## 2. Studied site and analytical methods

### 2.1. Studied site

In order to enlighten the very long-term corrosion mechanisms, it has been chosen to focus on a single site where numerous specimens submitted to multisecular indoor atmospheric corrosion could be sampled. All the studied samples came from the Amiens cathedral chain. This cathedral was built in the XIIIth century, but, in 1497 a reinforcement chain made of iron bars was put all around the Triforium [14] as can be seen on Fig. 1. The chain is constituted of 90 bars of 4 m long. 25 specimens of about 1 $cm^3$ were sampled all around the Triforium and 6 rust powder samples were scraped. Temperature ($T°$) and relative humidity (RH) variations were measured at different locations near the irons bars in the building during several months [15]. The results show very little variability of relative humidity and temperature inside, probably due to the thermal inertia of the cathedral.

### 2.2. Analytical methods

#### 2.2.1. Rust layer characterization

Samples were first mounted into cross sections in Mecaprex MA2 epoxy resin. They were polished with SiC abrasive papers (grades 800 to 4000) then using diamond paste (3 and 1 μm) under ethanol in order to avoid any phase transformation during preparation.

Micro X-ray diffraction analyses were performed in a transmission mode. Therefore, a specific sample preparation under thin films was required. Cross-sections were pasted on glass slides with a balsam (Crystal bond, BROT) soluble in acetone only. By polishing with SiC papers under ethanol, sample thickness was reduced to approximately 100 μm [4].

First observations were carried out using an optical microscope to obtain a general overview of the corrosion layout. Then chemical composition of the rust layers was determined by energy dispersive spectrometry (EDS) (SAMx IDFix software) coupled to a scanning electron microscope (SEM) (LEO 120, Cambridge Instruments, operating at 15 kV). The Si(Li) detector used for these EDS analyses was equipped with a thin beryllium window which allowed the detection and quantification of oxygen with a good accuracy (about 2 wt% relative error on iron oxides references).

In order to identify and locate the phases present in the rust layer, previous studies have shown that the coupling of micro Raman spectroscopy and micro-X-ray diffraction is very efficient [7]. Micro-Raman measurements were performed at the Laboratoire de Dynamique, Interaction et Réactivité (LADIR) with a micro-Raman Notch-based spectrometer LabRam Infinity (Jobin Yvon-Horiba) using a laser radiation at 532 nm. Samples were observed under an Olympus microscope with Olympus objectives 100 magnification, giving a beam waist diameter of about 3 μm. The spectrome-

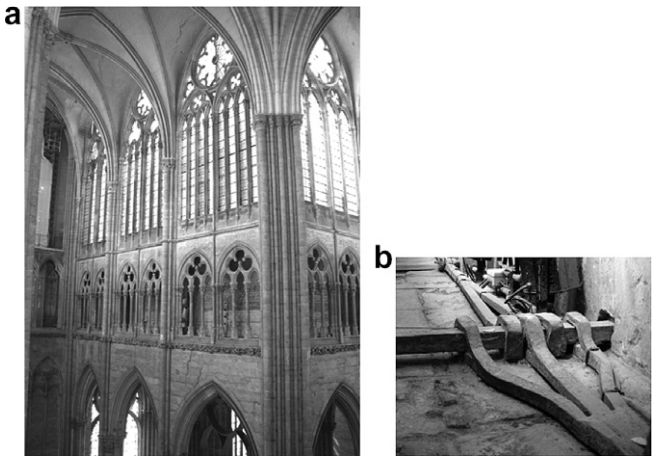


**Fig. 1.** Amiens cathedral; (a) triforium photograph; (b) iron chains placed around the Triforium.

ter setting offers a spectral resolution of about 2 $cm^{-1}$. As some iron oxides are highly sensitive to laser irradiation [16], measurements were always performed with a power at the sample surface kept below 100 μW in order to avoid any phase transformation. Phase identification was made by comparison with reference spectra [16,17]. Hyperspectral maps were also recorded on the sample in order to achieve a fine localisation of the oxidized phases [7]. In order to evaluate the reactive phase proportion, phase quantification is needed. Since phases are usually mixed in the analyzed volume in ancient rust layers, spectral decomposition is required. Consequently, hyperspectral maps were integrated in the CorAtmos program designed by D. Baron (LADIR). This program, based on a linear combination of reference 'pure' spectra [18], fits each experimental spectrum to obtain the phases proportion for each point of the analyzed area. Both the phase proportions and the quantitative mapping of a single phase in the rust layer can be deduced thanks to this program [19].

Micro X-ray diffraction (μXRD) analyses were performed on a photon microprobe built on a rotating anode X-ray generator. The beam delivered by a Molybdenum (Kα at 17.45 keV) anode was first monochromatised by a toroidal multilayer mirror and then focused on a surface of $20 \times 20\ \mu m^2$ through a borosilicate capillary. μXRD patterns were collected in transmission mode downstream the thin film sample by a 2D image plate detector. Classical $I = f(2\theta)$ powder μXRD patterns were obtained after circular integration of the diffracted image using the FIT2D program [20].

*2.2.2. Electrochemical measurements*

Part of the electrochemical measurements were performed at the Laboratoire Analyse et Modélisation pour la Biologie et l'Environnement (LAMBE) in a three electrodes cell. Reference electrode was an AgCl coated silver wire; the counter one was a platinum electrode. The working electrode was made of graphite powder mixed with the sample powder (80–20 wt%, respectively) compressed on a stainless steel grid. Electrolyte was a desaerated NaCl 0.1 M solution, with buffered pH at 7.5 (PIPES solution, 0.05 M) and maintained at 25 °C. Galvanostatic curves were recorded by imposing 25 μA/mg matter on Amiens cathedral chain rust powder.

The other part of the reduction experiments have been conducted in an electrochemical cell coupled to *in situ* X-ray absorption spectroscopy (XAS) and XRD characterization. Therefore a specific cell has been designed by the Laboratoire de Chimie du Solide Minéral (LCSM). It is constituted of three parts, as is schematized on Fig. 2(a): a body, a conductive part that comes close to the body and enables to fix the working electrode and a piston that enables to get a very fine electrolyte layer on the sample surface.

This cell was working in transmission mode. Reference electrode was calomel one and the counter electrode was a platinum wire. A composite electrode made of graphite powder mixed with the sample powder fixed on amorphous carbon plate by conducting silver paint constituted the working electrode. As for the measurements in the lab cell, the electrolyte was a desaerated NaCl 0.1 M solution, but in this case the pH was buffered at 9.5 (TAPS solution, 0.05 M) in order to increase the reduction rate. Potentiostatic curves were recorded by imposing −900 mV versus $E_{ref}$. This cell was used in two experiments set-ups:

- Energy dispersive X-ray absorption spectroscopy was performed on ID-24 beamline at ESRF in transmission mode, as presented on Fig. 2(b). The energy scans were performed using energy dispersive optics. A polychromatic fan of radiation from two undulators was diffracted by a polychromator crystal, and vertically and horizontally focused down to a $50 \times 100\ \mu m^2$ spot on the sample. A position sensitive detector allowed to collect in parallel a whole absorption spectrum leading to msec time resolution. This configuration ensured very quick acquisition and enabled to obtain an accurate temporal resolution of the reduction reaction. A metallic Fe foil provided energy calibration of the monochromator.
- In addition, X-ray diffraction experiments have been conducted at Pierre Süe laboratory, under the macroscopic beam of the rotating anode generator (Molybdenum, Kα at 17.45 keV) with an Image Plate detector.

## 3. Results and discussion

### 3.1. Sample characterization by coupled micro-beam techniques

*3.1.1. Physico-chemical analysis on archaeological artefacts*

The average thickness of the corrosion layer observed on historical samples was between 100 and 300 μm (Fig. 3(a)). Some cracks were present, a part of them quite large (up to 50 μm), parallel or perpendicular to the metal/oxide interface. They could result from corrosion products growing. The corrosion system was constituted of a dark grey matrix in which some light grey zones were visible. They could sometimes be in contact with the metal core, but more often were dispersed in the rust layer. EDS analyses revealed, in addition to Fe and O, the presence of impurities. Calcium was a significant one, mainly located in cracks, where its amount could at-

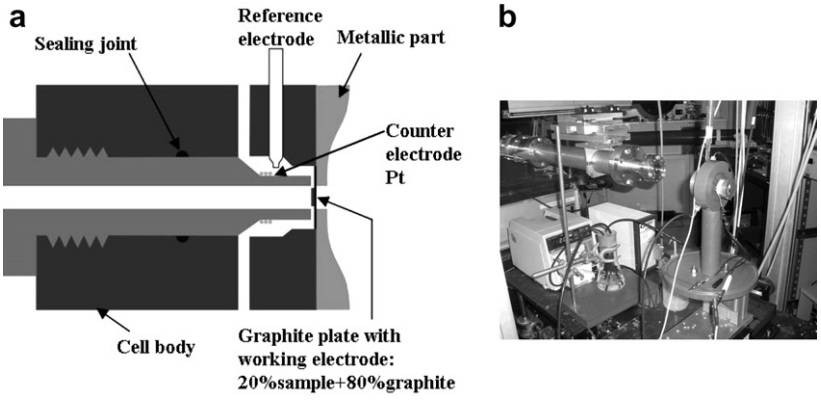


**Fig. 2.** (a) Electrochemical cell schematic view; (b) cell and its support on ID 24, ESRF.

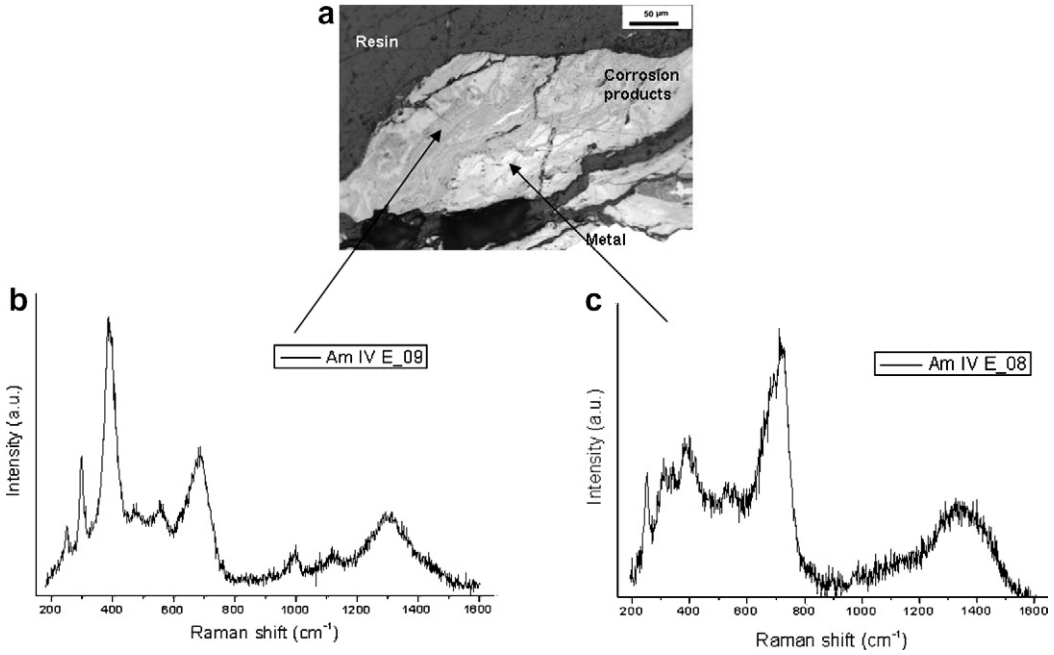


**Fig. 3.** Amiens cathedral chain rust layer; (a) optical micrograph of the rust layer; (b) goethite and (c) hydrated oxy-hydroxide Raman spectra (the narrowed peak around 250 $cm^{-1}$ underline the presence in the analysed volume of some Lepidocrocite) collected on archaeological sample Am IV E 110.

tempt about 4 wt%. Its presence could be correlated with calcium carbonate coming from the walls. Sulphur, silicon, phosphorus, chloride, sodium and magnesium were locally detected at a level lower than 0.5 wt%.

Micro-X-ray diffraction and micro-Raman analyses revealed the presence of goethite α-FeOOH as the most common phase in the rust layer. Lepidocrocite γ-FeOOH was also present, but locally and preferentially in the external zone of the corrosion layer. Akaganeite β-FeOOH was detected on 15 samples over 25 analyzed, in very localised spots near cracks or in the external zone. In addition to the identification and localisation of well-crystallized phases, analyses conducted with Raman micro-spectroscopy enabled to detect less crystallized phases (Fig. 3). Moreover, Raman micro-spectrometry giving a smaller beam than micro-XRD enabled to get a finer phase localisation in the rust layer. On spectra collected in lighter zones of the corrosion layer (Fig. 3(c)) a wide band around 700 $cm^{-1}$ was recorded. By comparison with reference spectra collected on synthesised powders, this kind of vibration band could be attributed to one of the following phases: poorly crystallized maghemite, feroxyhite or ferrihydrite [7]. All these poorly crystallized phases show a weak Raman diffusion. In addition during mapping exposure times were limited, consequently the obtained spectra were often poor quality ones. Under these conditions, it was tricky to distinguish between theses phases only using Raman mapping. Consequently, some isolated spectra were recorded with longer exposure time. They presented one single large band around 700 $cm^{-1}$ similar to the one observed for ferrihydrite or feroxyhite. On the contrary, the maghemite spectrum presented two shoulders on the broad band at 670 and 720 $cm^{-1}$. The light grey marblings observed on historical samples were therefore associated to a poorly crystallized ferrihydrite or feroxyhite phase. To ensure this result, some experiments of X-ray Absorption spectroscopy under synchrotron radiation have been performed and the results are under analysis.

As a conclusion, chemical and structural analyses revealed nearly the same rust layer general layout for all samples: a matrix composed of goethite with other phases locally present, lepidocrocite, akaganeite and what seemed to be a type of ferrihydrite or feroxyhite, as presented on Fig. 4.

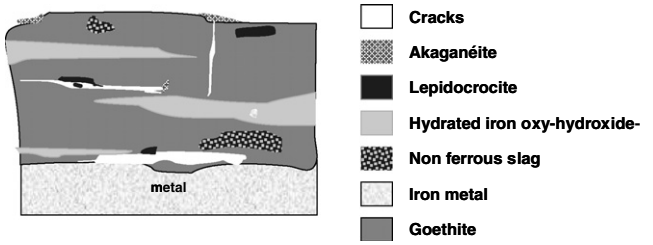


**Fig. 4.** Schematic view of the corrosion layer developed on the Amiens cathedral chain.

*3.1.2. Toward a 'semi-quantification' of phase proportions in the rust layer*

The CorAtmos program described in the experimental section was applied to the hyperspectral maps to extract quantitative information. First, a pure reference spectra database was set up, in which four groups of phases were discriminated:

- Goethite, as a stable phase
- Akaganeite, as a chlorine containing phase
- Lepidocrocite, as an active phase
- And the poorly crystallized hydrated iron III oxy-hydroxides, as very reactive phases.

Goethite spectra recorded in ancient samples exhibit variations related to various state of crystallinity. However, whatever its crystallinity, goethite was considered as a stable phase. Thus, it was decided as a first approach to group the different existing types of goethite under one single group. For this quantification in terms of reactivity, all poorly crystallized hydrated iron III oxy-hydroxides were also regarded as a single group.

The treatment of Raman spectra obtained on phase mixes by linear combination of pure phases presents some limitations, because the reference spectrum set did not reproduce the whole variability of encountered spectra. However, this limitation was overcome by considering a phase differentiation into reactivity families. In this view, the proportions of reactivity groups obtained

were satisfying ones and this work aimed towards a statistical picture of the entire corrosion system. Until now, the procedure was applied to four samples with 4–7 hyperspectral images gathered on each sample to ensure a statistical view. The quantitative maps obtained for the oxidized phases (Fig. 5) were in good agreement with the schematic rust layer description observed with Raman mapping.

Then, sector diagrams representing the proportion of each phase in the rust layer could be plotted (Fig. 6). The four samples already studied enabled to draw first conclusions. Goethite and the poorly crystallized iron III oxy-hydroxide were the main phases in the rust layer, followed by lepidocrocite with very low quantities of akaganeite. Some little variability in the phase proportions could also be noted, especially for the goethite and the akaganeite phases.

Considering the proportion of active and non-active phases, the evaluation of the whole layer reactivity could be proposed through this semi-quantification program.

### 3.2. Electrochemical studies

#### 3.2.1. Electrochemical study of ancient rust layers

In addition, the reduction reactivity of rust layer powders was investigated and compared to the results already obtained for such samples by Antony et al. [21,22]. The obtained curves $E = f(Q)$ presented on Fig. 7(a) showed some variability. In order to quantify these variations, a 'reduction reactivity ratio' was calculated, following the equation (2):

$$x = \frac{Q_{\text{experimental}}}{Q_{\text{theoretical}}} \tag{2}$$

where $Q_{\text{experimental}}$ is the exchanged charge during reduction, and $Q_{\text{theoretical}}$ is the theoretical charge that would be observed if all the iron III present in the sample could be reduced, assuming in a first approach that the global composition of all rust samples is FeOOH. Values obtained for Amiens cathedral were compared with other one already published [22] (Fig. 7(b)). This comparison pointed out a decrease of the reactivity ratio with the samples age.

#### 3.2.2. Reduction of ferric phases during the wetting stage

Lepidocrocite, feroxyhite and ferrihydrite were supposed to be reduced during the first part of the wet–dry cycle. To study the reduction behaviour of these different phases, experiments in an electrochemical cell coupled to *in situ* characterization by XAS and XRD were performed. In a first stage, only results obtained on lepidocrocite will be presented in the following paragraphs.

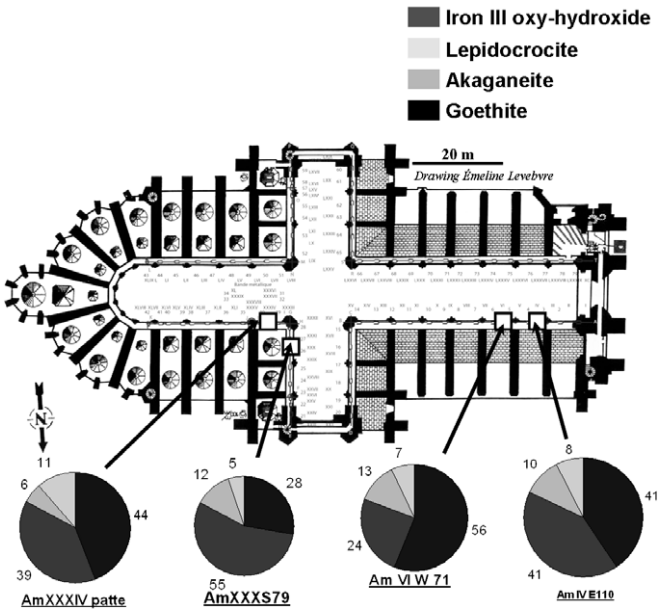


**Fig. 6.** Sector diagrams of four samples placed around the cathedral map.

For both couplings, acquisitions were done before, during and after the reduction process. The initial and final X-ray absorption near edge structure (XANES) spectra recorded during the reduction of lepidocrocite phase are presented on Fig. 8. The energy shift of the edge from 7128 eV to lower energies (Fig. 8) indicated a decrease of the oxidation state. The comparison with an iron II phase seemed to prove that the reduced phase contains at least a part of iron II species. Marked oscillations after the edge indicated also that the reduced compound is locally organised.

X-ray diffraction patterns obtained before and after the reduction process under X-ray diffraction are presented on Fig. 9. Lepidocrocite could be easily identified on the initial diagram (Fig. 9(a)). Two intense peaks were also present, linked to the graphite powder used to make the working electrode. On the final diagram, as for XAS experiment, it was clearly shown that lepidocrocite has totally disappeared and that a new phase was appearing at the end of the reduction process.

From the initial and final X-ray diffraction patterns, the interetricular distances of both lepidocrocite and the reduced phase have been extracted (Table 1). A comparison was done with JCPDF database and the best coincidence was found with a mix of $Fe(OH)_2$ and

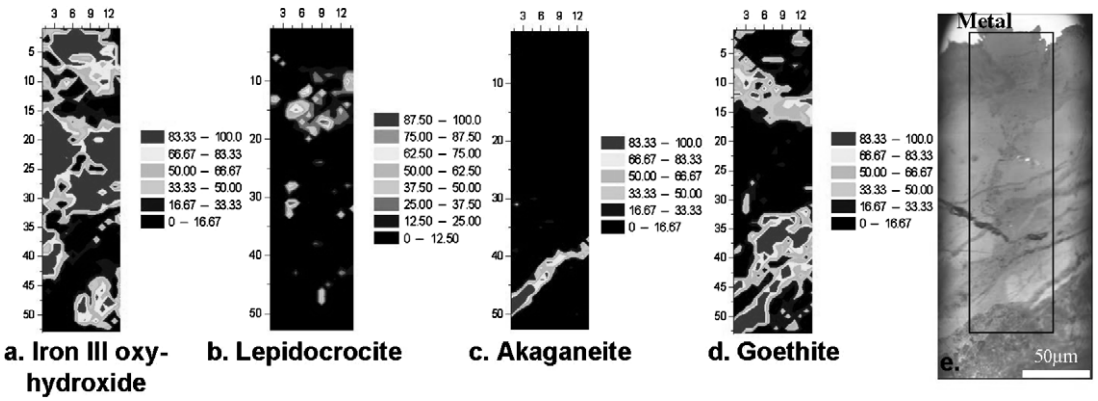


**Fig. 5.** (a) to (d) Quantitative location map from the CorAtmos program; e image of the scanned area. Sample AmXXX S79 (Raman hyperspectral map: 14 × 53 pixel and 5 µm step, so 756 spectra, 300 s each).

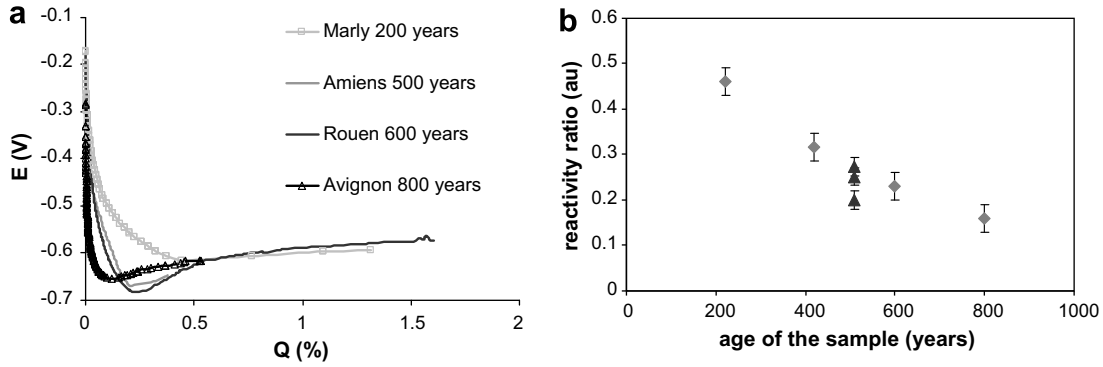


**Fig. 7.** (a) Reduction curves of ancient samples coming from different French cities; (b) Reactivity ratio evolution versus sample age; Antony [21] (diamonds), this study (triangles).

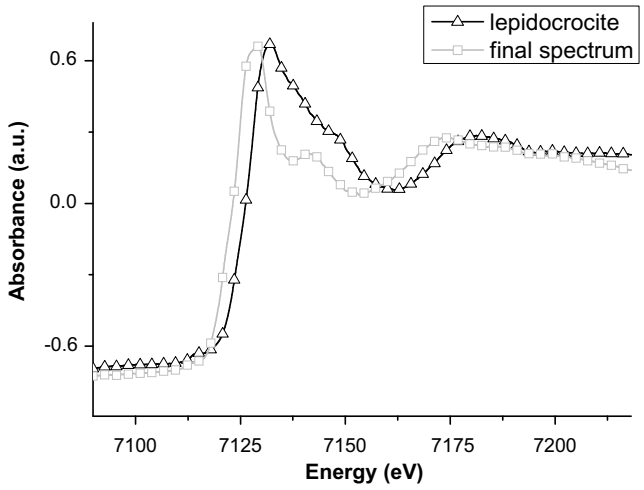


**Fig. 8.** XANES initial and final spectra.

**Table 1**
Intereticular distances for lepidocrocite and the reduced phase

| Lepidocrocite | Reduced phase |
|---|---|
| 6.30645 | 6.7601 |
| 3.00857 | 4.58504 |
| 2.48634 | 2.7612 |
| 2.37579 | 2.55567 |
| 1.95662 | 2.4207 |
| 1.53867 | 1.80262 |
| 1.44346 | 1.68992 |
| 1.3845 | 1.63058 |
| | 1.59855 |
| | 1.5455 |
| | 1.49823 |
| | 1.35205 |
| | 1.20433 |

$Fe(OH)_3$ files (see also Fig. 9(b)). The peak occurring at $2\theta = 6.7$ could belong to a third phase not identified yet. Further exploitation of XAS and XRD results have to be done in order to refine the structure of the reduced phase.

## 4. Conclusion

Several samples coming from the indoor atmospheric corrosion site of the Amiens cathedral have been characterized through coupling between micro-focused techniques. A schematic view of the corrosion layer has been drawn, with a goethite matrix crossed by hydrated iron oxy-hydroxide marblings. Lepidocrocite was detected in locally places, as well as akaganeite. A semi-quantification of phases function of their reactivity was achieved and enables to evaluate roughly the reactivity of the rust layer, coupled with the study of its electrochemical response. The CorAtmos program pointed out large amounts of poorly crystallized phase of type ferrihydrite and/or feroxyhite in the corrosion system. These results have to be taken into account for a further modelling of corrosion processes to improve Stratmann based modelling considering only the lepidocrocite phase.

Moreover, reduction reaction of the lepidocrocite phase was studied in specific conditions. It enabled to evidence an iron II intermediate during the corrosion mechanisms. To go further in this way, the reduction experiments done on lepidocrocite have to be realized with ferrihydrite and ferroxyhite reference powder, to demonstrate that these phases can be reduced in atmospheric

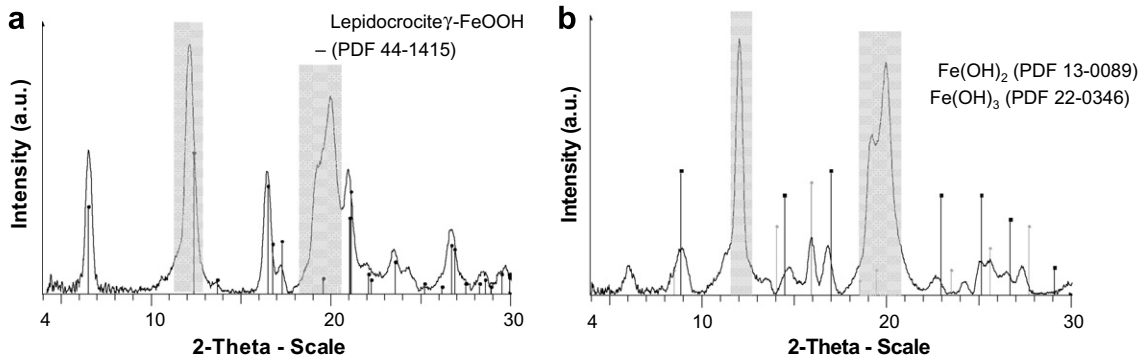


**Fig. 9.** (a) XRD initial spectrum before lepidocrocite reduction; the graphite peaks are marked in grey; (b) XRD final spectrum after reduction and nearest JCPDF files.

corrosion conditions. Then an archaeological powder itself could be tested. Different pH conditions could also been investigated to ensure a good correlation between laboratory experiments and natural conditions.

As another perspective, cathodic site location for oxygen reduction in the second step of the wet–dry cycle will be of great importance for the modelling of corrosion mechanisms. All these results would help the design of nuclear waste overpacks. They could also be used in the field of built heritage in order to propose a reliable diagnosis of degradation in iron-bearing monuments.

## Acknowledgements

The authors would like to thank the architects, historians and archaeologists who gave the access to the samples and were implicated in this study, particularly Maxime L'Heritier (LPS), Arnaud Thimbert (Université Lille1) and Ms Emeline Lefebvre (Université Lille1).

The authors would like also to thank Gemma Guillera (ID24, ESRF) for her precious help in time resolved XAS experiments.

This work was founded by the French program ANR ARCOR, the GdR Chim'Art and the PNRC 'Corrosion Atmosphérique' of French Ministry of Culture.

## References

[1] Journal Officiel. 124e année 1 (1991).
[2] U.R. Evans, C.A.J. Taylor, Corros. Sci. 12 (1972) 227.
[3] P. Dillmann, V. Vigneau, F. Mazaudier, C. Blanc, S. Hoerle. Rust characterisation of ancient ferrous artefact exposed to indoor atmospheric corrosion, in: Prediction of Long Term Corrosion Behaviour in Nuclear Wastes System, European Federation of Corrosion, Cadarache, France, 2003
[4] S. Réguer, P. Dillmann, F. Mirambet, Corros. Sci. 49 (2007) 2726.
[5] P. Dillmann, F. Mazaudier, S. Hoerle, Corros. Sci. 46 (2004) 1401.
[6] T. Misawa, K. Asami, K. Hashimoto, S. Shimodaira, Corros. Sci. 14 (1974) 279.
[7] D. Neff, L. Bellot-Gurlet, P. Dillmann, S. Reguer, L. Legrand, J. Raman Spectrosc. 37 (2006) 1228.
[8] M. Stratmann, Metallurgica I Odlewnictwo 16 (1990) 46.
[9] M. Stratmann, K. Hoffmann, Corros. Sci. 29 (1989) 1329.
[10] S. Hoerlé, F. Mazaudier, P. Dillmann, G. Santarini, Corros. Sci. 46 (2004) 1431.
[11] M. Yamashita, H. Miyuki, Y. Matsuda, H. Nagano, T. Misawa, Corros. Sci. 36 (1994) 283.
[12] H. Kihira, T. Misawa, T. Kusunoki, K. Tanabe, T. Saito, Corros. Eng. 48 (1999) 979.
[13] V. Lair, H. Antony, L. Legrand, A. Chausse, Corros. Sci. 48 (2006) 2050.
[14] E. Lefebvre, La place et le rôle des métaux dans l'architecture gothique à travers l'exemple de la cathédrale d'Amiens. Étude de cas: le chaînage du triforium de la cathédrale d'Amiens., in: Archéologie médiévale, Master 1, Amiens, 2006, p. 127.
[15] J. Monnier, D. Neff, P. Dillmann, I. Guillot, E. Rocca, F. Mirambet, The long term atmospheric corrosion of iron: influence of constitutive phases of the corrosion layers, in: Eurocorr 2007, Freiburg, 2007.
[16] D. Neff, S. Reguer, L. Bellot-Gurlet, P. Dillmann, R. Bertholon, J. Raman Spectrosc. 35 (2004) 739.
[17] S. Réguer, D. Neff, L. Bellot-Gurlet, P. Dillmann, J. Raman Spectrosc. 38 (2007) 389.
[18] F. Salpin, F. Trivier, S. Lecomte, C. Coupry, J. Raman Spectrosc. 37 (2006) 1403.
[19] J. Monnier, D. Baron, D. Neff, L. Bellot-Gurlet, P. Dillmann. Studying long term indoor atmospheric corrosion mechanisms on archaeological iron artefacts. Insight by Raman imaging and towards a semi-quantitative composition of rust layers, in: IVth International Conference on the Application of Raman Spectroscopy in Art and Archaeology, Modena (Italie), 2007.
[20] A.P. Hammersley, ESRF International report No EXP/AH/93-02. (1993).
[21] H. Antony, Etude électrochimique des composés du fer - Apport à la compréhension des processus environnementaux, Thèse, Evry, 2005. p. 213.
[22] H. Antony, S. Perrin, P. Dillmann, L. Legrand, A. Chaussé, Electrochim. Acta. 52 (2007) 7754.